

Bose-Einstein condensation of magnons in Cs₂CuCl₄: a dilute gas limit near the saturation magnetic field

D.L. Kovrizhin^{1,3}, V. Yushankhai^{2,4}, L. Siurakshina⁴

¹Max-Planck-Institute für Physik Komplexer Systeme, Nöthnitzer Str. 38, 01187 Dresden, Germany

²Max-Planck-Institute für Chemical Physik Fester Stoffe, Nöthnitzer Str. 40, 01187 Dresden, Germany

³Russian Research Centre Kurchatov Institute, Kurchatov sq. 1, 123182 Moscow, Russia

⁴Joint Institute for Nuclear Research, 141980 Dubna, Russia

Based on a realistic spin Hamiltonian for a frustrated quasi-two dimensional spin-1/2 antiferromagnet Cs₂CuCl₄, a three-dimensional spin ordering in the applied magnetic field B near the saturation value B_c is studied within the magnon Bose-Einstein condensation (BEC) scenario. With the use of a hard-core boson formulation of the spin model, a strongly anisotropic magnon dispersion in Cs₂CuCl₄ is calculated. In the dilute magnon limit near B_c , the hard-core boson constraint is resulted in an effective magnon interaction which is treated in the Hartree-Fock approximation. The critical temperature T_c is calculated as a function of a magnetic field B and compared with the phase boundary $T_c(B)$ experimentally determined in Cs₂CuCl₄ [Phys. Rev. Lett. **95**, 127202 (2005)].

I. INTRODUCTION

The insulator Cs₂CuCl₄ is a quasi-two dimensional spin-1/2 antiferromagnet (AFM) composed of triangular lattices (bc -plane) which are weakly coupled along crystallographic a -direction.¹ In spite of a low spin, low dimensionality and geometrical frustration of spin interactions, a three-dimensional (3D) magnetic long-range ordering occurs in Cs₂CuCl₄ at sufficiently low temperatures $T \lesssim T_N \simeq 0.6\text{K}$. In the ordered state, magnetic moments lie in an easy bc -plane and form an incommensurate spiral structure.¹ An easy-plane spin anisotropy in Cs₂CuCl₄ is produced by a Dzyaloshinskii-Moriya (DM) interaction with a DM vector $\vec{D} \parallel \vec{a}$. The anisotropy breaks SU(2) symmetry, however, U(1) symmetry corresponding to spin rotations around \vec{D} vector is still present. The applied magnetic field $\vec{B} \parallel \vec{a}$ preserves U(1) symmetry and causes the spiral spin order to develop into a cone spin structure with increasing B : a longitudinal spin component grows with B , while a spiral transverse component decreases steadily and disappears completely at a saturation field B_c . For higher fields, $B > B_c$, the Zeeman interaction overcomes the antiferromagnetic spin coupling and the system enters a field-induced ferromagnetic state.² In this state, *ferromagnetic* magnons become elementary spin excitations with a gapped spectrum and a quadratic energy dispersion near magnon band minima. In the opposite direction, i.e. by starting from a high field $B > B_c$ and passing through B_c , one finds a reversed behavior: the field-induced magnon gap disappears at B_c and a spiral transverse magnetic ordering develops below B_c . This ordered state is characterized by a gapless spin excitation spectrum with a linear low-energy dispersion.

Such a phase transition observed^{2,3} in Cs₂CuCl₄ in the applied magnetic field $\vec{B} \parallel \vec{a}$ in a vicinity of B_c can be regarded as a Bose-Einstein condensation (BEC) of a dilute gas of magnons.^{4,5} This suggestion was confirmed experimentally and supported theoretically in Ref. 3. In this context, two particular features of Cs₂CuCl₄ have to be

mentioned. First, because of a rather weak dominant exchange coupling $J \simeq 4.3\text{K}$ in this material, an exceptionally low saturation field $B_c \simeq 8.5\text{T}$ can be easily achieved. Second, because of the extremely strong anisotropy of the ferromagnetic magnon spectrum in Cs₂CuCl₄, 3D quadratic magnon dispersion is seen at very low energies $E < E^* \simeq 50\text{mK}$, and for $E > E^*$ the actual magnon spectrum is of 2D character. Therefore, an access to very low temperatures $T \sim 50\text{mK}$ is required to be as close as possible to the asymptotic regime where universal 3D scaling laws are expected to hold.

Cs₂CuCl₄ is an easy-plane quantum AFM with a gapless spin excitation spectrum at zero magnetic field.¹ Up to now, most of studies of a magnon (triplon) BEC have been reported^{6,7,8,9,10} on TlCuCl₃ and BaCuSi₂O₆ that belong to a more rare class of gapped AFMs. In these materials, a transverse spin long-range ordering occurs in the field range $B_{c1} < B < B_{c2}$. In TlCuCl₃ and BaCuSi₂O₆, a saturation field B_{c2} is rather high $\sim 50\text{T}$, which makes an observation of a magnon BEC at B_{c2} a complicated matter, while lower fields near B_{c1} are accessible. Within the 3D magnon BEC scenario,^{11,12,13} near B_{c1} the ordering temperature $T_c(B)$ is described by a power-law $T_c(B) \sim (B - B_c)^{1/\phi}$ with a universal critical exponent $\phi_{BEC} = 3/2$. A few experimental findings show, however, that the observed in TlCuCl₃ phase transition deviates from a pure magnon BEC: first, an anisotropic spin coupling (of unknown nature) might break the axial U(1) symmetry of the system and produce a small but finite spin gap^{14,15,16} in the ordered state at $B > B_{c1}$ and, second, the reported critical exponent ϕ is somewhat larger than predicted by theory.⁷ Magnetic properties of BaCuSi₂O₆ are suggested to be well described by a quasi-two dimensional isotropic Heisenberg model and the reported¹⁰ recently convergence of the measured exponent ϕ to the predicted value $\phi_{BEC} = 3/2$ is in accord with the 3D magnon BEC scenario.

In this paper a theoretical description of the magnon BEC transition in Cs₂CuCl₄ near the saturation field is

presented with more details as compared to the previous work.³ In section II, a model spin Hamiltonian applicable to Cs_2CuCl_4 is discussed and rewritten in the hard-core boson representation. Two branches of the bare magnon dispersion and their densities of states are calculated. In section III, the hard-core boson constraint is treated in ladder approximation and the Bethe-Salpeter equation is solved to calculate the effective magnon interaction in the dilute gas limit. In the next section IV, the obtained effective interaction is considered in a mean-field approximation and the leading effects of magnon interaction are extracted and discussed. In section V, the critical temperature $T_c(B)$ as a function of applied magnetic field is calculated and compared both with the predicted universal behavior of the phase boundary^{11,12,13} near B_c and with experimental data. Short concluding remarks can be found in section VI.

II. SPIN HAMILTONIAN AND MAGNON DISPERSION

The spin Hamiltonian \mathcal{H} of Cs_2CuCl_4 involves the isotropic exchange \mathcal{H}_0 , the DM anisotropic term \mathcal{H}_{DM} and the Zeeman energy \mathcal{H}_B . By using the notations of Ref. 17, the isotropic part \mathcal{H}_0 can be written as

$$\mathcal{H}_0 = \sum_{\mathbf{R}} [J \vec{S}_{\mathbf{R}} \vec{S}_{\mathbf{R}+\tau_1+\tau_2} + J' (\vec{S}_{\mathbf{R}} \vec{S}_{\mathbf{R}+\tau_1} + \vec{S}_{\mathbf{R}} \vec{S}_{\mathbf{R}+\tau_2}) + J'' \vec{S}_{\mathbf{R}} \vec{S}_{\mathbf{R}+\tau_3}], \quad (1)$$

where the nearest neighbor vectors τ_1 and τ_2 are indicated in Fig. 1 and the out-of-plane vector τ_3 connects spins on vertical bonds between adjacent layers. A small relative shift of adjacent layers is neglected. Within each

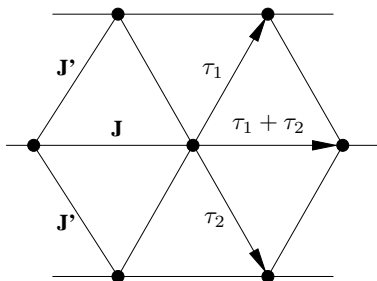


FIG. 1: Fragment of the triangular lattice (bc -plane) with nearest-neighbor exchange couplings, J and $J' \approx J/3$. The Dzyaloshinskii-Moriya coupling \mathcal{D} is on the same zig-zag bonds as the exchange J'

layer, the dominant exchange J distinguishes a chain direction and the DM interaction is situated on interchain zig-zag bonds

$$\mathcal{H}_{DM} = \sum_{\mathbf{R}} (-1)^n \vec{D} \vec{S}_{\mathbf{R}} \times [\vec{S}_{\mathbf{R}+\tau_1} + \vec{S}_{\mathbf{R}+\tau_2}]. \quad (2)$$

The crystallographic \vec{a} -direction is chosen to be \vec{z} axis and because $\vec{D} = (0, 0, \mathcal{D})$ the bc -plane becomes the easy plane for the ground state spin alignment in zero magnetic field. In Eq. (2) a layer index n is introduced to show that DM vectors alternate between adjacent layers. In the present study we consider the applied magnetic field $\vec{B} \parallel \vec{a}$ and Zeeman energy reads

$$\mathcal{H}_B = -g\mu_B B \sum_{\mathbf{R}} S_{\mathbf{R}}^z, \quad (3)$$

where $g \simeq 2.2$ and μ_B is the Bohr magneton. The spin coupling parameters determined with high accuracy by neutron scattering measurements² are: $J = 4.34\text{K}$, $J'/J = 0.34$, $J''/J = 0.045$ and $\mathcal{D}/J = 0.053$. The total Hamiltonian \mathcal{H} has $U(1)$ symmetry arising from spin rotations around \vec{z} axis. In Cs_2CuCl_4 the saturation field $B_c \simeq 8.5\text{T}$ and for $B > B_c$ at zero temperature the spins are fully polarized. To consider the magnetic phase transition in the vicinity of B_c and at low T , we use the hard-core boson representation for spin-1/2 operators. Two types of bosons $a_{\mathbf{R}}$ and $b_{\mathbf{R}'}$ are introduced for even and odd layers, respectively. This is given with a replacement $S_{\mathbf{R}}^+ \rightarrow a_{\mathbf{R}}$, $S_{\mathbf{R}}^- \rightarrow a_{\mathbf{R}}^+$ and $S_{\mathbf{R}}^z = 1/2 - a_{\mathbf{R}}^+ a_{\mathbf{R}}$ in even layers and the same transformation leads to $b_{\mathbf{R}'}$ for \mathbf{R}' belonging to odd layers. Such a replacement must be complemented by a constraint of no sites with boson occupancies higher than unity. The constraint is satisfied by adding to \mathcal{H} an infinite on-site repulsion, $\mathcal{U} \rightarrow \infty$, among the bosons

$$\mathcal{H}_U^{(a)} + \mathcal{H}_U^{(b)} = \mathcal{U} \sum_{\mathbf{R}} a_{\mathbf{R}}^+ a_{\mathbf{R}}^+ a_{\mathbf{R}} a_{\mathbf{R}} + \mathcal{U} \sum_{\mathbf{R}'} b_{\mathbf{R}'}^+ b_{\mathbf{R}'}^+ b_{\mathbf{R}'} b_{\mathbf{R}'}. \quad (4)$$

In the reciprocal space with an orthogonal basis we choose the Brillouin zone with wave-vectors restricted to $0 \leq q_x < 2\pi$, $0 \leq q_y < 4\pi$, and $0 \leq q_z < 2\pi$, and define Fourier transforms of boson operators

$$a_{\mathbf{q}} = \frac{1}{\sqrt{\mathcal{N}}} \sum_{\mathbf{R}} a_{\mathbf{R}} e^{-i\mathbf{q}\mathbf{R}}, \quad b_{\mathbf{q}} = \frac{1}{\sqrt{\mathcal{N}}} \sum_{\mathbf{R}'} b_{\mathbf{R}'} e^{-i\mathbf{q}\mathbf{R}'}, \quad (5)$$

where $\mathcal{N} = N/2$ and N is the total number of the spin-1/2 lattice sites in the system. Fourier transforms of spin interactions now read

$$J_{\mathbf{q}} = J \cos q_x + 2J' \cos(q_x/2) \cos(q_y/2),$$

$$J''_{\mathbf{q}} = J'' \cos(q_z/2), \quad (6)$$

$$\mathcal{D}_{\mathbf{q}} = 2\mathcal{D} \sin(q_x/2) \cos(q_y/2).$$

Two branches of 2D noninteracting magnons are described by the energy dispersions

$$\varepsilon_{\mathbf{q}}^{a,b} = J_{\mathbf{q}} \mp \mathcal{D}_{\mathbf{q}} + \Delta\varepsilon, \quad (7)$$

where $\Delta\varepsilon = g\mu_B B - (J + 2J' + J'')$. With these notations, the bilinear part of the total Hamiltonian takes the

form

$$\mathcal{H}_{bil} = \sum_{\mathbf{q}} [\varepsilon_{\mathbf{q}}^a a_{\mathbf{q}}^+ a_{\mathbf{q}} + \varepsilon_{\mathbf{q}}^b b_{\mathbf{q}}^+ b_{\mathbf{q}} + J_{\mathbf{q}}'' (a_{\mathbf{q}}^+ b_{\mathbf{q}} + b_{\mathbf{q}}^+ a_{\mathbf{q}})], \quad (8)$$

and leads to two 3D magnon branches, \mathcal{A} and \mathcal{B} with bare dispersions

$$\varepsilon_{\mathbf{q}}^{\mathcal{A},\mathcal{B}} = J_{\mathbf{q}} \mp \text{sign} \mathcal{D}_{\mathbf{q}} \sqrt{\mathcal{D}_{\mathbf{q}}^2 + J_{\mathbf{q}}''^2} + \Delta\varepsilon. \quad (9)$$

The degenerate minima $\varepsilon_{\mathbf{Q}_1}^{\mathcal{A}} = \varepsilon_{\mathbf{Q}_2}^{\mathcal{B}}$ are at $\mathbf{Q}_1 = (\pi + \delta_1, 0, 0)$ for branch \mathcal{A} and at $\mathbf{Q}_2 = (\pi - \delta_2, 2\pi, 0)$ for branch \mathcal{B} . Without losing precision we can use $\delta_1 \approx \delta_2 \approx \delta = 2 \arcsin(J'/2J)$. The bilinear part of \mathcal{H} now reads

$$\mathcal{H}_{bil} = \sum_{\mathbf{q}} [(E_{\mathbf{q}}^{\mathcal{A}} - \mu_0) \mathcal{A}_{\mathbf{q}}^+ \mathcal{A}_{\mathbf{q}} + (E_{\mathbf{q}}^{\mathcal{B}} - \mu_0) \mathcal{B}_{\mathbf{q}}^+ \mathcal{B}_{\mathbf{q}}], \quad (10)$$

where

$$\begin{pmatrix} \mathcal{A}_{\mathbf{q}} \\ \mathcal{B}_{\mathbf{q}} \end{pmatrix} = \begin{pmatrix} \alpha_{\mathbf{q}} & \beta_{\mathbf{q}} \\ -\beta_{\mathbf{q}} & \alpha_{\mathbf{q}} \end{pmatrix} \begin{pmatrix} a_{\mathbf{q}} \\ b_{\mathbf{q}} \end{pmatrix}, \quad (11)$$

$$\alpha_{\mathbf{q}} = \sqrt{\frac{1}{2} \left[1 + \frac{|\mathcal{D}_{\mathbf{q}}|}{\sqrt{\mathcal{D}_{\mathbf{q}}^2 + J_{\mathbf{q}}''^2}} \right]}, \quad (12)$$

$$\beta_{\mathbf{q}} = -\text{sign} \mathcal{D}_{\mathbf{q}} \sqrt{\frac{1}{2} \left[1 - \frac{|\mathcal{D}_{\mathbf{q}}|}{\sqrt{\mathcal{D}_{\mathbf{q}}^2 + J_{\mathbf{q}}''^2}} \right]},$$

and

$$\begin{aligned} E_{\mathbf{q}}^{\mathcal{A}} &= \varepsilon_{\mathbf{q}}^{\mathcal{A}} - \varepsilon_{\mathbf{Q}_1}^{\mathcal{A}}, \\ E_{\mathbf{q}}^{\mathcal{B}} &= \varepsilon_{\mathbf{q}}^{\mathcal{B}} - \varepsilon_{\mathbf{Q}_2}^{\mathcal{B}}. \end{aligned} \quad (13)$$

In Eq. (10), the bare chemical potential of magnons $\mu_0 = -[\varepsilon_{\mathbf{Q}_1}^{\mathcal{A}} + \Delta\varepsilon] = -[\varepsilon_{\mathbf{Q}_2}^{\mathcal{B}} + \Delta\varepsilon]$ can be written as $\mu_0 = g\mu_B(B_c - B)$, which defines a saturation field $B_c = W/(g\mu_B)$. Here the magnon bandwidth W is a function of spin coupling parameters J, J', J'' and \mathcal{D} . In terms of J , $W = 2.898J$ and therefore $B_c = 8.51\text{T}$, assuming $g = 2.2$.

Due to the symmetry property of two magnon branches $E_{\mathbf{Q}_1+\mathbf{q}}^{\mathcal{A}} = E_{\mathbf{Q}_2-\mathbf{q}}^{\mathcal{B}}$, their densities of states (DOS) coincide, $\rho^{\mathcal{A}}(E) = \rho^{\mathcal{B}}(E)$, where

$$\rho^{\mathcal{A},\mathcal{B}}(E) = \frac{1}{N} \sum_{\mathbf{q}} \delta(E - E_{\mathbf{q}}^{\mathcal{A},\mathcal{B}}). \quad (14)$$

The upper end of the calculated DOS is at $E_u = W$. For our purposes, the most important is the low-energy part of $\rho^{\mathcal{A},\mathcal{B}}(E)$ depicted in Fig. 2. A critical point in the magnon spectrum is clearly seen at $E = E^* \simeq 50\text{mK}$: 3D character of the spectrum at $E < E^*$ changes into 2D one for $E > E^*$.

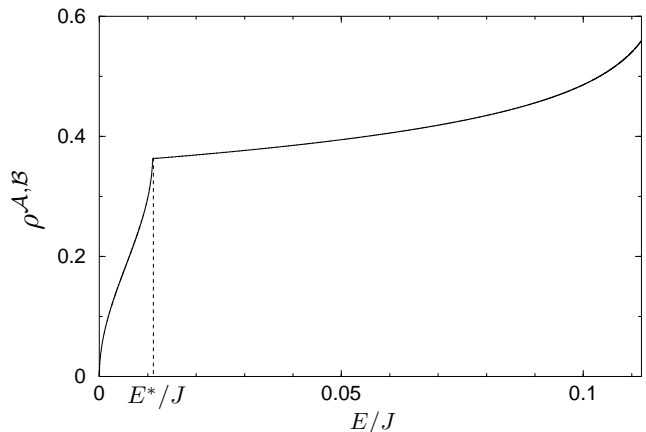


FIG. 2: Low-energy part of magnon density of states (in units $1/J$) for \mathcal{A} and \mathcal{B} branches.

III. EFFECTIVE MAGNON INTERACTION

When treating the magnon interactions, we take into account the dominant, $\mathcal{U} \rightarrow \infty$, hard-core repulsion and neglect effects of a \mathbf{q} -dependent part of interaction. Then, $\mathcal{H}_{int} \simeq \mathcal{H}_{\mathcal{U}}^{(a)} + \mathcal{H}_{\mathcal{U}}^{(b)}$, where

$$\begin{aligned} \mathcal{H}_{\mathcal{U}}^{(a)} + \mathcal{H}_{\mathcal{U}}^{(b)} &= \\ \frac{\mathcal{U}}{N} \sum_{\substack{\mathbf{q}_1, \mathbf{q}_2, \\ \mathbf{q}_3, \mathbf{q}_4}} (a_{\mathbf{q}_1}^+ a_{\mathbf{q}_2}^+ a_{\mathbf{q}_4} a_{\mathbf{q}_3} + b_{\mathbf{q}_1}^+ b_{\mathbf{q}_2}^+ b_{\mathbf{q}_4} b_{\mathbf{q}_3}) \Delta_{\mathbf{q}_1+\mathbf{q}_2, \mathbf{q}_3+\mathbf{q}_4}, \end{aligned} \quad (15)$$

and $\Delta_{\mathbf{q}_1+\mathbf{q}_2, \mathbf{q}_3+\mathbf{q}_4}$ implies the momentum conservation $\mathbf{q}_1 + \mathbf{q}_2 = \mathbf{q}_3 + \mathbf{q}_4$. Below we refer to $\mathcal{H}_{\mathcal{U}}^{(a)}$ and $\mathcal{H}_{\mathcal{U}}^{(b)}$ as the hard-core magnon repulsion in a and b channels, respectively.

In high magnetic field, $B > B_c$, a fully spin polarized state is the vacuum state for magnons. Upon decreasing field, in the very vicinity of B_c , i.e. $B \lesssim B_c$ and at low temperature the number of magnons is very small, $n \sim (1 - B/B_c)$. In this case an effective magnon interaction can be found as a result of multiple magnon scattering by summing up ladder diagrams.¹⁸ When accomplishing such a summation, we neglect interference between a and b channels. In this approximation, the problem reduces to solving the similar Bethe-Salpeter equation for the renormalized scattering amplitudes $\Gamma^{(a)}$ and $\Gamma^{(b)}$ in both channels. Therefore, below we discuss with more detail the channel a .

By substituting the transformation $a_{\mathbf{q}} = \alpha_{\mathbf{q}} \mathcal{A}_{\mathbf{q}} - \beta_{\mathbf{q}} \mathcal{B}_{\mathbf{q}}$ into interaction Hamiltonian $\mathcal{H}_{\mathcal{U}}^{(a)}$ in Eq. (15) one finds that $\mathcal{H}_{\mathcal{U}}^{(a)}$ splits into sixteen scattering terms. In each process, the bare interaction acquires now an extra factor given by a product of four $\alpha_{\mathbf{q}}$ and $\beta_{\mathbf{q}}$ coefficients. For instance, a scattering process $(\mathcal{A}_{\mathbf{q}_3}, \mathcal{B}_{\mathbf{q}_4}) \rightarrow (\mathcal{A}_{\mathbf{q}_1}, \mathcal{B}_{\mathbf{q}_2})$ is described by the amplitude $2\alpha_{\mathbf{q}_1}\beta_{\mathbf{q}_2}\alpha_{\mathbf{q}_3}\beta_{\mathbf{q}_4}\mathcal{U}$. Taking into account multiple magnon scattering in the ladder ap-

proximation leads to a replacement of $2\mathcal{U}$ by an effective two-particle interaction $\Gamma^{(a)}(\mathbf{K}, \omega)$, where $\mathbf{K} = \mathbf{q}_1 + \mathbf{q}_2 = \mathbf{q}_3 + \mathbf{q}_4$ and $\omega = \omega_1 + \omega_2 = \omega_3 + \omega_4$ are the total momentum and energy of a scattering magnon pair; the extra factor remains unchanged. The same holds for the other fifteen scattering processes. In the magnetic field close to B_c and at low T only the particles near the magnon band minima at $\mathbf{q} = \mathbf{Q}_{1,2}$ are present, which allows us to send $\omega \rightarrow 0$ and consider $\Gamma^{(a)}(\mathbf{K}, 0) \equiv \Gamma_{\mathbf{K}}^{(a)}$.

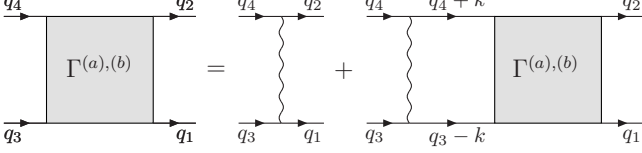


FIG. 3: Bethe-Salpeter equation for the scattering vertices $\Gamma^{(a),(b)}$

The effective interaction $\Gamma_{\mathbf{K}}^{(a)}$ is obtained in an explicit form by solving the Bethe-Salpeter equation presented in Fig. 3 diagrammatically. In this presentation, $q_i = (\mathbf{q}_i, \omega_i)$ and $k = (\mathbf{k}, \omega')$ are four-dimensional vectors. Any external incoming or outgoing line is associated with either \mathcal{A} or \mathcal{B} magnon; two internal lines labelled by $q_4 + k$ and $q_3 - k$ correspond to Green's function $\mathcal{G}^{(a)}(q \pm k) = \alpha_{q \pm k}^2 \mathcal{G}^{(\mathcal{A})}(q \pm k) + \beta_{q \pm k}^2 \mathcal{G}^{(\mathcal{B})}(q \pm k)$. Here $\mathcal{G}^{(\mathcal{A})}(q \pm k)$ and $\mathcal{G}^{(\mathcal{B})}(q \pm k)$ are the Green's functions of decoupled \mathcal{A} and \mathcal{B} magnons. Since the bare interaction \mathcal{U} is \mathbf{q} - and ω -independent, the solution of the Bethe-Salpeter equation in the zero frequency limit is

$$[\Gamma_{\mathbf{q}_1 + \mathbf{q}_2}^{(a)}]^{-1} = \frac{1}{\mathcal{N}} \sum_{\mathbf{k}} \left[\frac{\alpha_{\mathbf{q}_1 + \mathbf{k}}^2 \alpha_{\mathbf{q}_2 - \mathbf{k}}^2}{E_{\mathbf{q}_1 + \mathbf{k}}^{\mathcal{A}} + E_{\mathbf{q}_2 - \mathbf{k}}^{\mathcal{A}}} + \frac{\alpha_{\mathbf{q}_1 + \mathbf{k}}^2 \beta_{\mathbf{q}_2 - \mathbf{k}}^2}{E_{\mathbf{q}_1 + \mathbf{k}}^{\mathcal{A}} + E_{\mathbf{q}_2 - \mathbf{k}}^{\mathcal{B}}} + \frac{\beta_{\mathbf{q}_1 + \mathbf{k}}^2 \alpha_{\mathbf{q}_2 - \mathbf{k}}^2}{E_{\mathbf{q}_1 + \mathbf{k}}^{\mathcal{B}} + E_{\mathbf{q}_2 - \mathbf{k}}^{\mathcal{A}}} + \frac{\beta_{\mathbf{q}_1 + \mathbf{k}}^2 \beta_{\mathbf{q}_2 - \mathbf{k}}^2}{E_{\mathbf{q}_1 + \mathbf{k}}^{\mathcal{B}} + E_{\mathbf{q}_2 - \mathbf{k}}^{\mathcal{B}}} \right]. \quad (16)$$

The similar derivation applies also to an effective magnon interaction $\Gamma_{\mathbf{q}_1 + \mathbf{q}_2}^{(b)}$ in the channel b , which can be obtained merely from $\Gamma_{\mathbf{q}_1 + \mathbf{q}_2}^{(a)}$ by interchanging $\mathcal{A} \leftrightarrow \mathcal{B}$.

By collecting back all the terms in both a and b channels, one arrives at an effective interaction Hamiltonians of magnons. It becomes clear now that the effective Hamiltonian takes the original form (15) where the bare parameter $2\mathcal{U}$ has to be replaced by $\Gamma_{\mathbf{q}_1 + \mathbf{q}_2}^{(a)}$ and $\Gamma_{\mathbf{q}_1 + \mathbf{q}_2}^{(b)}$ in channel a and b , respectively.

IV. MEAN-FIELD THEORY

The main goal of the present study is to calculate a shape of the phase boundary, i.e. a field dependence of the critical temperature $T_c(B)$ for $B \lesssim B_c$. When approaching B_c from below, $T_c \rightarrow 0$. In the low- T region near B_c , only low-energy magnon states at the band

minima wave-vectors $\mathbf{q} = \mathbf{Q}_1, \mathbf{Q}_2$ are occupied and contribute to the phase transition. In this section, we consider first how the magnon spectrum near the band minima is renormalized due to the effective magnon interaction. The study is based on the Hartree-Fock (HF) approximation, since near the quantum critical point, $B = B_c$ and $T = 0$, the HF theory is suggested to describe correctly the phase boundary.^{12,13}

We assume that the temperature approaches T_c from above. Then in the disordered phase, the mean-field interaction Hamiltonian in the channel a can be written as

$$\mathcal{H}_{int, MF}^{(a)} \simeq \frac{2}{\mathcal{N}} \sum_{\mathbf{q}_1, \mathbf{q}_2} \Gamma_{\mathbf{q}_1 + \mathbf{q}_2}^{(a)} \langle a_{\mathbf{q}_1}^+ a_{\mathbf{q}_1} \rangle a_{\mathbf{q}_2}^+ a_{\mathbf{q}_2}, \quad (17)$$

which is approximated further as follows

$$\begin{aligned} \Gamma_{\mathbf{q}_1 + \mathbf{q}_2}^{(a)} \langle a_{\mathbf{q}_1}^+ a_{\mathbf{q}_1} \rangle &\simeq \Gamma_{\mathbf{Q}_1 + \mathbf{q}_2}^{(a)} \alpha_{\mathbf{Q}_1}^2 \langle \mathcal{A}_{\mathbf{q}_1}^+ \mathcal{A}_{\mathbf{q}_1} \rangle \\ &+ \Gamma_{\mathbf{Q}_2 + \mathbf{q}_2}^{(a)} \beta_{\mathbf{Q}_2}^2 \langle \mathcal{B}_{\mathbf{q}_1}^+ \mathcal{B}_{\mathbf{q}_1} \rangle \\ &- \alpha_{\mathbf{q}_1} \beta_{\mathbf{q}_1} \Gamma_{\mathbf{q}_1 + \mathbf{q}_2}^{(a)} \langle \mathcal{A}_{\mathbf{q}_1}^+ \mathcal{B}_{\mathbf{q}_1} + \mathcal{B}_{\mathbf{q}_1}^+ \mathcal{A}_{\mathbf{q}_1} \rangle. \end{aligned} \quad (18)$$

In this expression, we made replacements $\Gamma_{\mathbf{q}_1 + \mathbf{q}_2}^{(a)} \alpha_{\mathbf{q}_1}^2 \rightarrow \Gamma_{\mathbf{Q}_1 + \mathbf{q}_2}^{(a)} \alpha_{\mathbf{Q}_1}^2$ and $\Gamma_{\mathbf{q}_1 + \mathbf{q}_2}^{(a)} \beta_{\mathbf{q}_1}^2 \rightarrow \Gamma_{\mathbf{Q}_2 + \mathbf{q}_2}^{(a)} \beta_{\mathbf{Q}_2}^2$, since the low-energy magnon densities $\langle n_{\mathbf{q}}^{\mathcal{A}} \rangle = \langle \mathcal{A}_{\mathbf{q}}^+ \mathcal{A}_{\mathbf{q}} \rangle$ and $\langle n_{\mathbf{q}}^{\mathcal{B}} \rangle = \langle \mathcal{B}_{\mathbf{q}}^+ \mathcal{B}_{\mathbf{q}} \rangle$ are located in the \mathbf{q} -space near \mathbf{Q}_1 and \mathbf{Q}_2 for \mathcal{A} and \mathcal{B} branch, respectively. Because of a symmetry of the magnon interaction, the band minima degeneracy is preserved and one has $\frac{1}{\mathcal{N}} \sum_{\mathbf{q}} \langle n_{\mathbf{q}}^{\mathcal{A}} \rangle = \frac{1}{\mathcal{N}} \sum_{\mathbf{q}} \langle n_{\mathbf{q}}^{\mathcal{B}} \rangle = n$. A possible shift due to magnon interaction of the band minima location in the \mathbf{q} -space at $\mathbf{Q}_{1,2}$ is assumed to be small and neglected below. In the zero-order approximation, the quantities $\langle \mathcal{A}_{\mathbf{q}_1}^+ \mathcal{B}_{\mathbf{q}_1} + \mathcal{B}_{\mathbf{q}_1}^+ \mathcal{A}_{\mathbf{q}_1} \rangle$ vanish, and we omit them in Eq. (18) as well. A validity of the latter approximation will be verified later on.

Similar arguments as above allow us to approximate the operator part in Eq. (17) as follows

$$\begin{aligned} a_{\mathbf{q}}^+ a_{\mathbf{q}} &\simeq \alpha_{\mathbf{Q}_1}^2 \mathcal{A}_{\mathbf{q}}^+ \mathcal{A}_{\mathbf{q}} + \beta_{\mathbf{Q}_2}^2 \mathcal{B}_{\mathbf{q}}^+ \mathcal{B}_{\mathbf{q}} \\ &- \alpha_{\mathbf{q}} \beta_{\mathbf{q}} (\mathcal{A}_{\mathbf{q}}^+ \mathcal{B}_{\mathbf{q}} + \mathcal{B}_{\mathbf{q}}^+ \mathcal{A}_{\mathbf{q}}), \end{aligned} \quad (19)$$

and to treat the effective magnon interaction in the channel b in the same manner as in the channel a . Finally, by noting that $\alpha_{\mathbf{Q}_1}^2 = \alpha_{\mathbf{Q}_2}^2 = \alpha^2$, $\beta_{\mathbf{Q}_1}^2 = \beta_{\mathbf{Q}_2}^2 = \beta^2$ and $\alpha^2 \gg \beta^2$, we retain only the leading terms in the mean-field interaction Hamiltonian, which leads to the following result

$$\begin{aligned} \mathcal{H}_{int, MF}^{(a)} + \mathcal{H}_{int, MF}^{(b)} &= \\ &2\Gamma n \sum_{\mathbf{q}} (\mathcal{A}_{\mathbf{q}}^+ \mathcal{A}_{\mathbf{q}} + \mathcal{B}_{\mathbf{q}}^+ \mathcal{B}_{\mathbf{q}}) \\ &- 2n \sum_{\mathbf{q}} \Gamma'_{\mathbf{q}} (\mathcal{A}_{\mathbf{q}}^+ \mathcal{B}_{\mathbf{q}} + \mathcal{B}_{\mathbf{q}}^+ \mathcal{A}_{\mathbf{q}}), \end{aligned} \quad (20)$$

where

$$\Gamma = \alpha^4 \Gamma_{2\mathbf{Q}_1}^{(a)} = \alpha^4 \Gamma_{2\mathbf{Q}_2}^{(b)} \quad (21)$$

$$\Gamma'_{\mathbf{q}} = \alpha_{\mathbf{q}} \beta_{\mathbf{q}} [\Gamma_{\mathbf{Q}_1+\mathbf{q}}^{(a)} - \Gamma_{\mathbf{Q}_2+\mathbf{q}}^{(b)}]$$

According to Eq. (20), the bare chemical potential of magnons is renormalized

$$\mu_0 \rightarrow \mu_{eff} = \mu_0 - 2\Gamma n. \quad (22)$$

With the use of the definition (12) for $\alpha_{\mathbf{q}}$ and (16) for $\Gamma^{(a)}$, we obtain numerically the estimate $\Gamma \simeq 0.85J$. The second term in Eq. (20) generates magnon hybridization. This term shifts the bottom of the magnon band slightly down and leads to a weak mass enhancement of low-energy magnons. Both effects are proportional to n^2 and we omit them since $n \ll 1$ near T_c for $(B_c - B) \ll B_c$. In this region, the low-energy magnon \mathcal{A} and \mathcal{B} branches remain decoupled, which justifies an approximation made before.

V. CRITICAL TEMPERATURE $T_c(B)$ NEAR B_c

In the previous sections we obtained in the dilute magnon limit $n \ll 1$, and within the HF approximation that the leading, linear in n , effect of magnon interaction is a renormalization of the chemical potential, Eq. (22). In this section we calculate the critical temperature $T_c(B)$ of a magnon BEC transition as a function of B assuming that for given $B \lesssim B_c$ the temperature approaches the phase boundary from the normal phase.

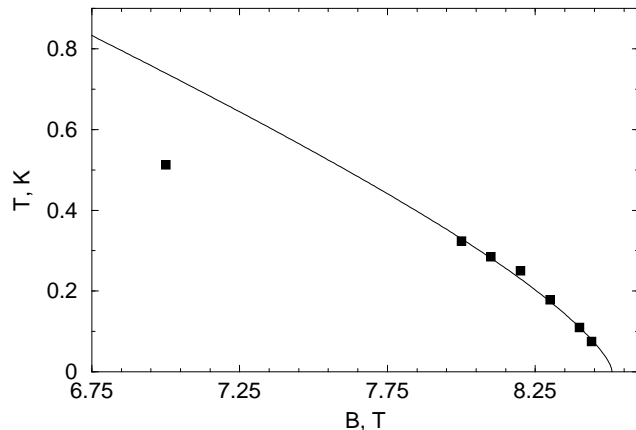


FIG. 4: Calculated phase boundary $T_c(B)$ near B_c (solid line). Experimental data (squares) are from specific heat measurements reported in Ref. 3

As follows from Eq.(22), a comparatively large magnon density n at high temperature makes the chemical potential to be negative, $\mu_{eff} < 0$, and all the magnons are noncondensed. Under decreasing T , μ_{eff} tends to zero and a BEC transition is expected to occur when $\mu_{eff} = 0$

at $T_c(B)$; for $T \leq T_c$, a condensate density n_0 starts to develop continuously at the magnon band minima. From Eq. (22), the condition for the phase transition is written as⁷

$$g\mu_B(B_c - B) = 2\Gamma n(T_c). \quad (23)$$

Here $n(T) = \mathcal{N}^{-1} \sum_{\mathbf{q}} f_B(E_{\mathbf{q}})$ with $f_B(E_{\mathbf{q}})$ being the Bose distribution function taken at $\mu_{eff} = 0$ and $E_{\mathbf{q}} = E_{\mathbf{q}}^{\mathcal{A}}$ or $E_{\mathbf{q}} = E_{\mathbf{q}}^{\mathcal{B}}$. This means that for $T < T_c$ the magnon condensate develops simultaneously at $\mathbf{q} = \mathbf{Q}_{1,2}$. Since at $\mu_{eff} = 0$ the distribution function $f_B(E)$ diverges as T/E for $E \rightarrow 0$, a magnon spectrum near the band minima mainly contribute to $n(T_c)$. If T_c is sufficiently low, the very low-energy magnons having a 3D quadratic dispersion dominate and drive the BEC transition. In this asymptotic regime the power-law is expected^{11,12,13} $T_c(B) \sim (B_c - B)^{1/\phi}$ with the universal exponent $\phi_{BEC} = 3/2$. To check this suggestion and to compare the calculated phase boundary with that determined experimentally in Cs_2CuCl_4 , we solved the equation (23) with the use of the magnon density of states, Fig. 2, realistic for Cs_2CuCl_4 . The result of calculations, with $B_c = 8.51\text{T}$ and $\Gamma = 0.85J$, is shown in Fig. 4 and compared with experimental data³ for $B \lesssim B_c$. In the very vicinity to B_c , the theoretical curve is well reproduced by the power-law with the calculated $\phi_{th} \simeq 1.5$, while a fit of experimental data yields³ $\phi_{exp} = 1.52(10)$; both values of the critical exponent are close to the universal $\phi_{BEC} = 3/2$.

VI. CONCLUSIONS

Based on a realistic quantum spin model in the hardcore boson representation, we developed a mean-field theory of a magnon BEC transition in Cs_2CuCl_4 near the saturation field B_c . The calculated critical temperature $T_c(B)$ describes surprisingly well the experimentally measured phase boundary in a narrow field region $B_c - \Delta B < B < B_c$, where $\Delta B/B_c \simeq 0.06$. In this region, where $0 \leq T_c < 300\text{mK}$, both the measured and calculated critical exponents ϕ are very close to the universal value $\phi_{BEC} = 3/2$ characteristic for 3D quadratic magnon dispersion. It means that in Cs_2CuCl_4 the magnon BEC near B_c is driven by 3D magnon states with energies below $E^* \approx 50\text{mK}$. Actually, by sending formally $E^* \rightarrow 0$ (see Fig. 2) in our calculations we obtained $T_c = 0$ at any B . At lower fields $B < B_c - \Delta B \simeq 8\text{T}$, a mean-field description of the experimentally determined phase boundary $T_c(B)$ fails, as was expected. Both thermal fluctuations and a temperature renormalization of the magnon spectrum have to be taking into account to improve a theoretical description of the phase boundary at lower magnetic fields.

VII. ACKNOWLEDGMENTS

We are grateful to D.Ihle, P.Thalmeier, M. Sigrist, and M.Vojta for many stimulating discussions. D.K. thanks

G.V.Pai and S.Sinha for helpful discussions. V.Y. acknowledges financial support by Deutsche Forschungsgemeinschaft.

-
- ¹ R. Coldea, D.A. Tennant, and Z. Tylczynski, Phys. Rev. B **68**, 134424 (2003)
- ² R. Coldea, D.A. Tennant, K. Habicht, P. Smeibidl, C. Wolters, and Z. Tylczynski, Phys. Rev. Lett. **88**, 137203 (2002)
- ³ T. Radu, H. Wilhelm, V. Yushankhai, D. Kovrizhin, R. Coldea, Z. Tylczynski, T. Lühmann, and F. Steglich, Phys. Rev. Lett. **95**, 127202 (2005)
- ⁴ T. Matsubara, and H. Matsuda, Prog. Theor. Phys. **16**, 569 (1956)
- ⁵ E.G. Batyev, and L.S. Braginskii, Sov. Phys. JETP **60**, 781 (1984)
- ⁶ A. Oosawa, M. Ishii, and H. Tanaka, J. Phys. Condens. Matter **11**, 265 (1999)
- ⁷ T. Nikuni, M. Oshikawa, A. Oosawa, and H. Tanaka, Phys. Rev. Lett. **84**, 5868 (2000)
- ⁸ G. Misguich and M. Oshikawa, J. Phys. Soc. Jpn. **73**, 3429 (2004)
- ⁹ M. Jaime *et al.*, Phys. Rev. Lett. **93**, 087203 (2004)
- ¹⁰ S.E. Sebastian *et al.*, cond-mat/0502374
- ¹¹ T. Giamarchi, and A.M. Tsvelik, Phys. Rev. B **59**, 11398 (1999)
- ¹² O. Nohadani, S. Wessel, B. Normand, and S. Haas, Phys. Rev. B **69**, 220402 (2004)
- ¹³ N. Kawashima, J. Phys. Soc. Jpn. **73**, 3219 (2004)
- ¹⁴ V.N. Glazkov, A.I. Smirnov, H. Tanaka, and A. Oosawa, Phys. Rev. B **69**, 184410 (2004)
- ¹⁵ A.K. Kolezhuk, V.N. Glazkov, H. Tanaka, and A. Oosawa, Phys. Rev. B **70**, 020403 (2004)
- ¹⁶ J. Sirker, A. Weisse, and O.P. Sushkov, J. Phys. Soc. Jpn. **74** Suppl., 129 (2005)
- ¹⁷ M.Y. Veillette, J.T. Chalker, and R. Coldea, cond-mat/0501347
- ¹⁸ A. Abrikosov, L. Gorkov, and T. Dzyaloshinskii, "Methods of quantum field theory in statistical physics", New York, Dover Publ. (1975)